33rd Annual International Conference of the IEEE EMBS
Boston, Massachusetts USA, August 30 - September 3, 2011

Analysis of the Vascular Sounds of the Arteriovenous Fistula's Anastomosis

Marco Munguía M.[1,2,*], Member, IEEE, and Bengt Mandersson[2]

Abstract— **In this paper, the vascular sounds of the arteriovenous fistula at the anastomosis and five centimeters downstream the anastomosis were analyzed. The analysis of the sounds was based on features extracted from the power spectral density (PSD) and wavelet decomposition. The database consists of 15 recordings at the anastomosis and 15 reference recordings obtained from 15 patients. The results showed that the vascular sounds at the anastomosis can be characterized as an extra energy in the higher frequencies (200-1000 Hz) i.e. higher mean frequency of the PSD than the reference recordings. Moreover, the wavelet decomposition of the anastomosis recordings showed a similar energy pattern, in the finer scales, to that found in studies of arterial and venous stenosis.**

I. INTRODUCTION

Vascular accesses are essential to provide hemodialysis treatment to patients suffering from end-stage renal disease. Among the possible vascular accesses, the arteriovenous (AV) fistula is the recommended choice due to its larger lifespan and low incidence of problems [1]. An AV fistula is created surgically and consists of the union of a vein and an artery. The connection is referred to as *anastomosis* and generally, it is located close to the patient's wrist or elbow.

When the vein is connected to the artery, the properties of the involved vessels are permanently altered [2], giving rise to a complex bio-fluid dynamic phenomenon. Many fluid dynamics investigations have been conducted in order to shed light on this phenomenon. In [3], [4], it has been studied the anastomosis geometry, specifically the influence of the angle on intimal hyperplasia development i.e. stenosis formation. A major finding was that at an angle of 10°, intimal thickening at the anastomotic floor (see Fig. 1) was observed and it was maximum when the angle was increased to 30°. On the contrary, when the angle was higher, 45° to 90°, thinning and dilatation of the vessel walls were observed.

In [5], a realistic model of the AV fistula was built to visualize the flow. They observed high wall shear stress values within 10 mm from the suture line which can be interpreted as an indicator of venous stenosis formation. Duplex and color-flow ultrasonography were used in [6] to suggest the three most common sites where stenotic lesions appear. It was not a surprise to find the anastomosis among them. However, it is important to note that not all stenotic lesions are progressive and in the case of the anastomosis, only a low percentage develops and therefore has medical implications.

On the other hand, phonoangiography (the quantitative analysis of sounds produced by blood flow) is a non-invasive and low cost technique that can be used for complementing current AV fistula monitoring methods such as physical examination and auscultation. The purpose of the present study is to analyze and characterize the phonoangiographic (PAG) signal of the arteriovenous fistula, specifically at anastomosis, in hemodialysis patients. For this purpose, acoustical features are extracted from the power spectral density (PSD) and wavelet decomposition. This paper is organized as follows. Section 2 presents a description of the dataset and the methods used to analyze the PAG signals. The results are described in section 3 and finally the conclusions are presented in section 4.

II. MATERIALS & METHODS

A. Database

The database consists of 30 recordings acquired from 15 patients undergoing hemodialysis treatment three times a week. The recordings were made in a secluded room 15 minutes before each patient's treatment was due to begin. During the data acquisition, the sampling frequency was set either to 2020 Hz or 10050 Hz. Thus, all signals were downsampled to 2 KHz. The transducer consisted of a microphone and a stethoscope head. The microphone was then connected to a Biopac system MP100 (BIOPAC Systems, Inc. USA). More details about the measuring setup can be found elsewhere [7]. The localization of the anastomosis was done by a nurse who located the thrill. The thrill is defined as: "a buzzing sensation that may be felt over the anastomosis" [8]. The reference recordings were obtained about five centimeters downstream the anastomosis location. Table 1 summarizes the database used in this study.

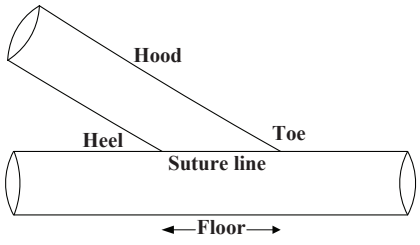

Fig. 1. Diagram of the anastomosis: Geometry nomenclature.

This work was supported by the Swedish International Development Cooperation Agency, Asdi

[1]UNI-Asdi-FEC Group, Faculty of Electrical Engineering and Computer Science, National University of Engineering, UNI, Managua, Nicaragua

[2]Signal Processing Group, Department of Electrical and Information Technology, Lund University, Lund, Sweden {mmm, Bengt.Mandersson}@eit.lth.se

*Corresponding author

B. Signal Processing

The different processing steps for the analysis of the PAG signal are presented in Fig. 2 and described in detail below. Since the recorded signals vary in amplitude, these were firstly normalized in amplitude. Then, a linear-phase, finite impulse response low-pass filter (3-dB filter cutoff frequency at 50 Hz) which estimates and subtracts the baseline wander from the sound recordings was implemented. Hereafter, the filtered signal will be referred to as $s(n)$. The envelope of the signal $s(n)$ was then calculated using the method described in [9], where the envelope is expressed as

$$x(n) = \sqrt{s^2(n) + \check{s}^2(n)}, \tag{1}$$

and $\check{s}(n)$ is the Hilbert transform of $s(n)$.

Then, the indexes of the maximum peaks of the envelope were determined for every heartbeat. The segmentation was performed on the signal $s(n)$. A cycle, $\bar{\mathbf{s}}_i$, was defined from 200 milliseconds before the maximum peak in the envelope to 200 milliseconds after the maximum peak i.e. L = 800 samples. Next, each extracted cycle was normalized in energy as follows

$$\mathbf{s}_i = \frac{\bar{\mathbf{s}}_i}{\sqrt{\sum_{i=1}^{L} \bar{\mathbf{s}}_i^2}}. \tag{2}$$

TABLE I
AV FISTULA TYPE, LOCATION AND DURATION OF THE SOUND RECORDINGS PER PATIENT

Subject	Type	Location	Signal	Duration
A	Brachial-cephalic	Anastomosis Reference	A_1 A_2	15 s 15 s
B	Brachial-cephalic	Anastomosis Reference	B_1 B_2	15 s 15 s
C	Radial-cephalic	Anastomosis Reference	C_1 C_2	30 s 30 s
D	Radial-cephalic	Anastomosis Reference	D_1 D_2	30 s 30 s
E	Radial-cephalic	Anastomosis Reference	E_1 E_2	10 s 10 s
F	Brachial-cephalic	Anastomosis Reference	F_1 F_2	10 s 10 s
G	Radial-cephalic	Anastomosis Reference	G_1 G_2	10 s 10 s
H	Radial-cephalic	Anastomosis Reference	H_1 H_2	10 s 10 s
I	Radial-cephalic	Anastomosis Reference	I_1 I_2	10 s 10 s
J	Radial-cephalic	Anastomosis Reference	J_1 J_2	10 s 10 s
K	Brachial-cephalic	Anastomosis Reference	K_1 K_2	10 s 10 s
L	Brachial-cephalic	Anastomosis Reference	L_1 L_2	10 s 10 s
M	Radial-cephalic	Anastomosis Reference	M_1 M_2	10 s 10 s
N	Radial-cephalic	Anastomosis Reference	N_1 N_2	10 s 10 s
O	Radial-cephalic	Anastomosis Reference	O_1 O_2	10 s 10 s

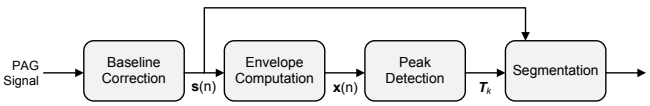

Fig. 2. Block diagram of the signal analysis framework used for the characterization of the vascular sounds.

C. Welch's Method

The Welch's method is a non-parametric technique used for estimating the power spectral based on the periodogram technique. It is carried out by dividing the time signal into successive blocks, forming the periodogram for each block, and averaging them [10]. Here, a windows size of 128 samples (64 milliseconds) and an overlapping of 50% were utilized. The mean frequency of the power spectral density (PSD) is defined as

$$\bar{w} = \frac{\int_o^\pi w\mathbf{S}(e^{jw})\mathrm{d}w}{\int_o^\pi \mathbf{S}(e^{jw})\mathrm{d}w}, \tag{3}$$

where $\mathbf{S}(e^{jw})$ is the estimated PSD.

D. Wavelet Decomposition

The Wavelet technique has been used successfully in many fields such as signal processing. It provides information on both frequency and time domain about the events in a signal. Wavelet is used here for characterization of the energy content in different frequency bands or scales [9]. Four levels of decomposition were selected. The frequency ranges for the different scales are shown in Table 2. Several types of wavelets were tested yielding no significant differences on the results. Finally, Daubachies type 4 wavelet was selected in this study.

Then, the four details wavelets coefficients (one per scale), $d_i(n)$, were calculated for each cycle. The scale energy SE_i is defined as,

$$SE_i = \sum d_i(n)^2. \tag{4}$$

A (base 2) logarithmic transformation was applied to the energy coefficients, since they presented a high dynamic range.

TABLE II
WAVELET DECOMPOSITION

Detail	Frequency Range in Hz	Time Resolution in milliseconds
1	500 - 1000	1
2	250 - 500	2
3	125 - 250	4
4	62.5 - 125	8

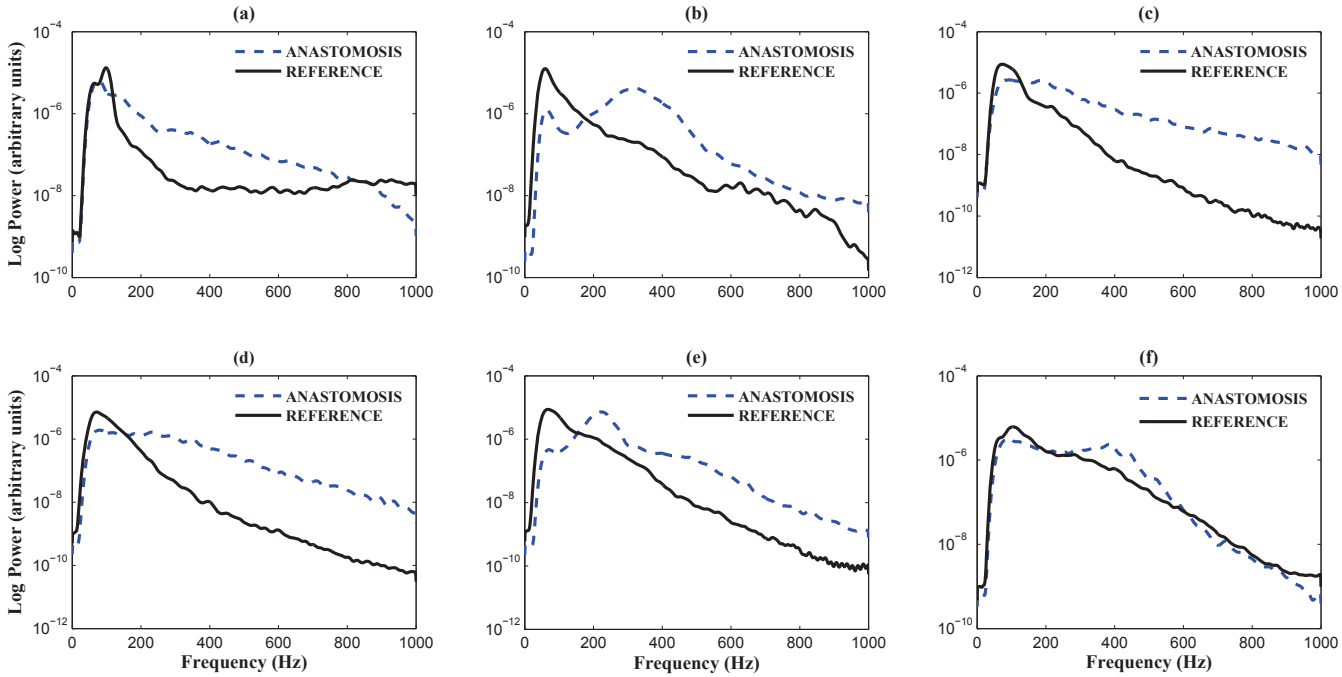

Fig. 3. Power Spectral Densities for both types of recordings of: (a) Patient A, (b) Patient C, (c) Patient G, (d) Patient H, (e) Patient M, and (f) Patient I. The PSD of the anastomosis recordings showed lower magnitude in the low frequency band and greater magnitude in the high frequency band than the reference recordings.

III. RESULTS

Since the power spectral densities and wavelet energy coefficients showed some slight variations from cycle to cycle. The averages of these features are reported per patient in order to obtain representative information.

A. Power Spectral Density Analysis

Power spectral densities for both types of recordings of six patients are shown in Fig. 3. Even though, the shape of the spectra from the anastomosis differs among the patients, the PSD of the anastomosis recordings can be broadly classified in two categories. In the first category, the PSD shows the behavior of a straight line with negative slope. Meanwhile, the second category shows a higher energy content in 200-500 Hz frequency band.

Furthermore, when the PSD of the anastomosis and reference recordings were compared, the spectral changes were clear. The PSD of the anastomosis recordings shows lower magnitude in the low frequency band and greater magnitude in the high frequency band than the reference recordings. To evaluate these differences in a quantitative manner, the mean frequency, $\bar{w}$, of the power spectrum was computed. The results of $\bar{w}$ are shown in Fig. 4. The $\bar{w}$ was significantly higher for the anastomosis recordings than the reference recordings (p = 0.0001, Wilcoxon rank sum test). The outliers in Fig. 4 correspond to patient J (anastomosis recording) and patient N (reference recording). In the case of patient J, the results of $\bar{w}$ were very low for both recordings and lower than the median $\bar{w}$ of the reference recordings. Since the fistula was only 17 days old, it is very plausible that the fistula was still in the maturation stage i.e. the process of vein wall thickening and increasing vein diameter due to the pressure of the artery inflow [8]. For patient N, the results of $\bar{w}$ were practically similar for both recordings and very close to the median $\bar{w}$ of the anastomosis recordings. In [5], it was shown that at a distance of 7 cm from the anastomosis, the relative turbulence intensity was still significant. Thus, it is very likely that the 5 cm distance between both measurement points was not enough and therefore, both recordings belong to the same class.

B. Wavelet Analysis

Principal component analysis and the sequential forward selection algorithm were helpful in selecting the best coefficients where the energy content differ the most. The energy in scale 1, SE_1, and scale 2, SE_2, were found to be the best selection. This seems to be reasonable since these coefficients contain high frequency information and that region is where energy, due to turbulent blood flow, is expected to be located. Figure 5 shows the scatter plot of the selected coefficients for all patients. Two well separated clusters are distinguished. The high energy cluster comprises mainly of anastomosis recordings. Meanwhile, the low energy cluster comprises mainly of reference recordings (p = 0.0009, 0.00003 for SE_1 and SE_2 respectively, Wilcoxon rank sum test).

In summary, the thrill at the anastomosis and its corresponding sound can be characterized as an extra energy in the 200–1000 Hz frequency band. In addition, the energy pattern found with wavelet is very similar to that found in [11] for artery stenosis and in [12] for venous stenosis in

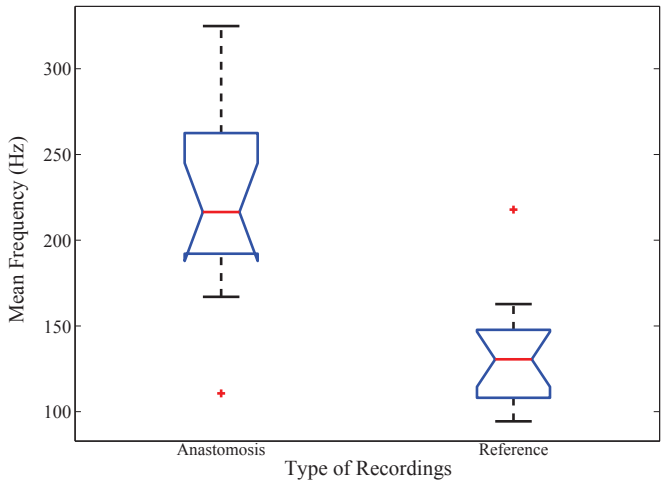

Fig. 4. Boxplot of the mean frequency, $\bar{w}$, for both types of recordings. The result of Wilcoxon rank sum test was **p = 0.0001**.

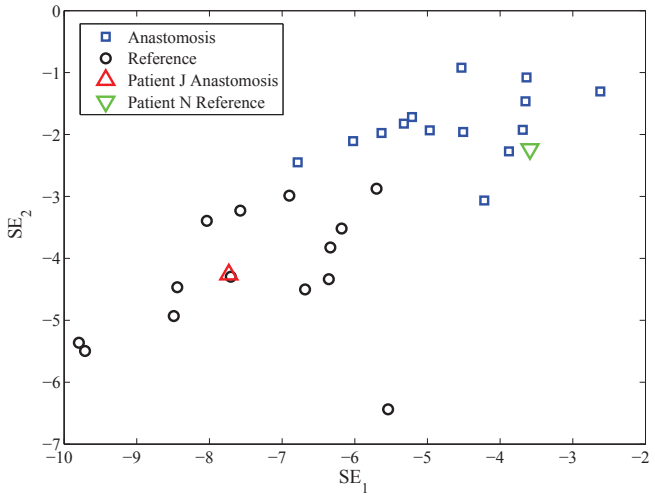

Fig. 5. Scatter plot of the SE_1 (x-axis) and SE_2 (y-axis) coefficients. Two well separated clusters can be distinguished. Greater energy content, in both scales, was found for the anastomosis recordings. The results of the Wilcoxon rank sum test were **p = 0.0009, 0.00003** for SE_1 and SE_2, respectively.

arteriovenous fistulas. These similarities may be due to the fact that the thrill also appears in cases of venous stenosis [8]. Thus, these results open the discussion about how similar are the vascular sounds generated at the anastomosis and a stenotic lesion? However, the answer to this question is out of the scope of the present study. It is also important to mention that none of the patients suffered from stenosis at the anastomosis at the time the recordings were made. Since the size of the database is small, the significance of these results needs to be further established on a larger dataset.

IV. CONCLUSIONS

In the present study, the vascular sounds generated at the anastomosis and downstream of the anastomosis were analyzed by mean of Welch's method and wavelet decomposition. The mean frequency of the power spectrum and details energy coefficients of the wavelet transform were used as parameters to indicate changes in the vascular sounds of the AV fistula. The results showed that although the shape of the spectrum varies from patient to patient for both types of recordings, the mean frequency was significantly greater for the anastomosis recordings than the reference recordings.

In addition, the results of wavelet decomposition showed that the differences in energy between both types of recordings were higher in the finer scales. Moreover, the energy pattern of the anastomosis recordings, in these scales, was very similar to that found in studies of venous and arterial stenosis. However, the significance of these results and their impact on a medical sense need to be further established.

V. ACKNOWLEDGEMENTS

The authors gratefully acknowledge Prof. Leif Sörnmo, Dr. Kristian Solem, Cecilia Nilsson and Andreas Larsson for providing the dataset used in this study.

REFERENCES

[1] NKF-K/DOQI, Clinical Practice Guidelines For Vascular Access: Update 2006, Am J Kidney Dis 2006 Jul;48 Suppl 1:S248-73

[2] M. S. Lemson, Intimal Hyperplasia in Prosthetic Vascular Access The Effect of Flow Variation and Anastomotic Geometry on its Development. University Hospital Maastricht, PhD thesis, 2000.

[3] R. S. Keynton, M. M. Evancho, R. L. Sims, N. V. Rodway, A. Gobin, and S. E. Rittgers, Intimal Hyperplasia and Wall Shear in Arterial Bypass Graft Distal Anastomoses: An *in vivo* Model Study, *Journal of Biomechanical Engineering*, vol. 123, 2001, pp. 464-473

[4] Z. S. Jackson, H. Ishibashi, A. I. Gotlieb, and B. L. Langille, Effects of Anastomotic Angle on Vascular Tissue Responses at End-to-Side Arterial Grafts, *Journal of Vascular Surgery*, vol. 34, 2001, pp. 300-307.

[5] S. Sivanesan, T. V. How, R. A. Black, and A. Bakran, Flow Patterns in the Radiocephalic Arteriovenous Fistula: An *in vitro* Study, *Journal of Biomechanics*, vol. 32, 1999, pp. 915-925.

[6] S. Sivanesan, T. V. How, and A. Bakran, Sites of Stenosis in AV fistulae for Haemodialysis Access, *Nephrology Dialysis Transplantation*, vol. 14, 1999, pp. 118-120.

[7] C. Nilsson and A. Larsson, *A Pilot Study of the Acoustical Properties of the Arteriovenous Fistula using Digital Signal Processing*, Department of Electroscience, Lund University, 2005.

[8] G. Beathard, A practitioner's Guide to Physical Examination of Dialysis Vascular Access, *Fistula First Project*, 2004.

[9] L. Sörnmo and P. Laguna, *Bioelectrical Signal Processing in Cardiac and Neurological Applications*, Elsevier/Academic Press, Amsterdam, The Netherlands, 2005.

[10] M. H. Hayes, *Statistical Digital Signal Processing and Modeling*, John Wiley and Sons, Inc., New York, 1996.

[11] Y. M. Akay, M. Akay, W. Welkowitz, S. Lewkowicz, and Y. Palti, Time-frequency Analysis of the Turbulent Sounds Caused by Femoral Artery Stenosis in Dogs Using Wavelet Transform, *Engineering in Medicine and Biology Society, Proceedings of the Annual International Conference of the IEEE*, vol. 6, 1992, pp. 2590-2591.

[12] P. Vásquez, M. Munguía M., and B. Mandersson, Arteriovenous Fistula Stenosis Detection using Wavelets and Support Vector Machines, *Proceedings of the 31st EMBS Annual International Conference*, 2009, pp. 5661-5664.